

ARTICLE MANUSCRIPT

## A generalized regionalization framework for geographical modelling and its application in spatial regression

Hao Guo<sup>a,b</sup>, Andre Python<sup>c</sup> and Yu Liu<sup>a,b</sup>

<sup>a</sup>Institute of Remote Sensing and Geographical Information Systems, School of Earth and Space Sciences, Peking University, Beijing, China; <sup>b</sup>Beijing Key Lab of Spatial Information Integration and Its Applications, Peking University, Beijing, China; <sup>c</sup>Center for Data Science, Zhejiang University, Hangzhou, China

### ARTICLE HISTORY

Compiled June 22, 2022

### ABSTRACT

In presence of spatial heterogeneity, models applied to geographic data face a trade-off between producing general results and capturing local variations. Modelling at a regional scale may allow the identification of solutions that optimize both accuracy and generality. However, most current regionalization algorithms assume homogeneity in the attributes to delineate regions without considering the processes that generate the attributes. In this paper, we propose a generalized regionalization framework based on a two-item objective function which favors solutions with the highest overall accuracy while minimizing the number of regions. We introduce three regionalization algorithms, which extend previous methods that account for spatially constrained clustering. The effectiveness of the proposed framework is examined in regression experiments on both simulated and real data. The results show that a spatially implicit algorithm extended with an automatic post-processing procedure outperforms spatially explicit approaches. Our suggested framework contributes to better capturing the processes associated with spatial heterogeneity with potential applications in a wide range of geographical models.

### KEYWORDS

Regionalization; spatial heterogeneity; geographical modelling; spatial regression

## 1. Introduction

Along with spatial dependency, spatial heterogeneity is one of the two fundamental properties of spatial data, commonly observed in both natural and social phenomena (Anselin 1988, Shaver 2005, Fotheringham and Sachdeva 2022). Spatial heterogeneity can be observed in the data, with a presence of heterogeneous attribute values across space, and in the processes that generate the data. In the presence of spatial heterogeneity, the estimated parameters of a given model or the specification of distinct models may vary across space. In contrast to physics or chemistry, principles and laws in social and environmental sciences usually do not hold across large spatial domains and scales. Replicability, which is the ability to obtain consistent results using similar data and methods, is therefore difficult to reach in geographic studies (Goodchild and Li 2021, Sui and Kedron 2021). Yet replicability may be partially achieved by allowing

some aspects of a geographical model (e.g. its estimated parameters) to vary across space, while keeping its structure (e.g. the set of features) replicable. This partial replicability refers to the concept of “weak replicability” (Goodchild and Li 2021, Liu *et al.* 2022).

A global model fitted for a whole study area may estimate an overall trend across space but cannot capture regional heterogeneity. In contrast, local models may explicitly account for spatial heterogeneity by allowing model parameters to vary across space. A well-known example is geographically weighted regression (GWR, Brunson *et al.* (1996)) and its extension, multiscale GWR (Fotheringham *et al.* 2017). In line with the concept of weak replicability (Goodchild and Li 2021), the model specification of GWR does not change in a study domain, but its parameters are allowed to vary across different locations within the study area. Yet the flexibility gained by representing geographical phenomena through local variations in the model parameters ineluctably affects the ability of local models to capture general patterns.

Regional models offer an intermediate approach positioned between global and local modelling<sup>1</sup>. In this framework, the study area is divided into a set of zones, which are usually required to be spatially contiguous, and a model is specified for each zone. The spatial contiguity constraint reflects the principle of spatial dependency formulated in Tobler’s first law of geography (Tobler 1970). Since near locations tend to exhibit similar geographical properties and processes, a regional aggregation of the spatial units may find a compromise between the accuracy and parsimony of the model.

However, delineating analytical regions is not trivial. The regionalization problem, formalized as the  $p$ -regions problem (Duque *et al.* 2011), aims to aggregate a set of spatial units into a predefined number of spatially contiguous regions, following optimization criteria. The mixed integer programming (MIP) approach may solve this problem exactly, yet it is computationally expensive and therefore only applicable to a relatively small number of spatial units (e.g.,  $5 \times 5$  grids) (Duque *et al.* 2011). Heuristic methods have been developed as a computationally-efficient alternative to exact procedures. This includes the automatic zoning procedure (AZP) (Openshaw 1977, Openshaw and Rao 1995), spatial ‘k’luster analysis by tree edge removal (SKATER) (Assunção *et al.* 2006), and regionalization with dynamically constrained agglomerative clustering and partitioning (REDCAP) (Guo 2008). A detailed comparison of these algorithms based on simulation experiments is provided in Aydin *et al.* (2021).

So far, regionalization algorithms have mostly focused on spatially constrained clustering, which aggregates data into regions with similar observed features without considering the underlying processes that generated the data. These descriptive approaches are unable to capture and quantify the role of potential drivers that may jointly lead, along with spatial dependency, to spatial clusters. These limitations are especially problematic in environmental and social studies, where the mechanisms leading to spatial clusters are often the result of complex factors. For example, the apparent effect of precipitation on plague intensity may change its direction between different regions due to unobserved factors. Rodent communities that transfer the disease may respond to precipitation differently, and hence, lead to variations in the observed effect of precipitation on plague intensity across space (Xu *et al.* 2011). In this case, simply considering similarity of explanatory factors in a phenomenon may not suffice to identify the described heterogeneity between regions.

We propose a generalized regionalization framework which can account for the geo-

---

<sup>1</sup>Throughout this paper, a regional model refers to a model which is applied in a region (a part of the study area).

graphical processes that generate the data and the associated regions, where spatially constrained clustering is a special case. Our framework can accommodate a large variety of geographic models, such as spatial linear regression, gravity models for spatial interaction data, or pixel-based classifier for remote sensing imagery. We introduce a two-item objective function which accounts for the trade-off between model precision and parsimony. If two regionalization schemes result in similar overall accuracy, the scheme with less regions is preferred. We compare the performance of three regionalization algorithms in their ability to reconstruct regions and maximizing accuracy. We consider one existing algorithm (AZP) and two extended algorithms based on K-Means and Regional-K-Means (Feng *et al.* 2021), which we entitled *K-Models* and *Regional-K-Models*. AZP does not require particular extension since it is suitable to a wide range of modelling scenarios. However, K-Means and Regional-K-Means algorithms are currently only applicable to spatially constrained clustering. Therefore, we extended them so that they can be applicable to a wider range of geographical models. We conduct experiments on both simulated and real datasets within a linear regression context, where the spatial units are aggregated based on processes that generate the data, specified in linear regression models, instead of the attribute values.

## 2. Related works

Regionalization can be viewed as a specific spatial clustering procedure aiming at aggregating spatial units into geographically connected regions (Wei *et al.* 2022). After the regionalization procedure, each unit is assigned to a unique region, and each region contains at least one unit (Duque *et al.* 2007). The number of regions is predefined in most methods, although some specific approaches treats it as an endogenous variable (Duque *et al.* 2012). The criteria used to identify the regions may include equity or threshold of attributes. For example, the population in each region should be as similar as possible or above a predefined value (Duque *et al.* 2012, Folch and Spielman 2014, Wei *et al.* 2021). Other criteria may include compactness of geometry (Li *et al.* 2014), spatial auto-correlation (Openshaw and Rao 1995), or fitness of a global model (Openshaw 1978). Note that our regional modelling approach differs from Openshaw (1978), where a global model is fitted and each region is treated as an individual observation. One common criterion is homogeneity, which assumes that spatial units in a region have similar properties. This is consistent with generic clustering analysis. Throughout the paper, we will consider the term “homogeneity” in a more general sense, which means robustness in the parameter estimation of a model across a region. For example, consider a simple linear regression model expressed as  $y_i = \beta_i x_i + \epsilon_i$ ,  $\epsilon_i \sim \mathcal{N}(0, \sigma_\epsilon^2)$ , with a dependent variable  $y_i$  and an independent variable  $x_i$  associated with a linear coefficient  $\beta_i$  allowed to vary for each spatial unit  $u_i$  within a region  $\mathcal{R}_j$  in a spatial domain  $\mathcal{D}$ . A region is considered homogeneous if, for each spatial unit, the estimated parameters are similar within  $\mathcal{R}_j$ . In other words, a region is homogeneous if  $\beta_i \approx \beta$ ,  $\forall u_i \in \mathcal{R}_j$ , which indicates similar relationship between  $y_i$  and  $x_i$  for all spatial units across the region. In practice a threshold can be set to determine a level of tolerance to assess similarity.

Let  $\mathbf{y}_i$  be the attribute vector associated with spatial unit  $u_i (i = 1, 2, \dots, N)$ . Current regionalization methods usually minimize an objective function of the sum of

within-region variability across all considered regions in  $\mathcal{D}$  (Equation 1):

$$\mathcal{L}(\mathcal{R}) = \sum_{j=1}^M \sum_{1 \leq i_1 < i_2 \leq N} I[u_{i_1}, u_{i_2} \in \mathcal{R}_j] \|\mathbf{y}_{i_1} - \mathbf{y}_{i_2}\|^2, \quad (1)$$

where  $\mathcal{L}(\mathcal{R})$  is the objective function associated with regions  $\mathcal{R} = \{\mathcal{R}_j\}_{j=1}^M$  in a spatial domain  $\mathcal{D}$ ;  $I[\text{cond}]$  is an indicator function, which takes 1 if condition (cond) is true, 0 otherwise;  $\|\cdot\|$  represents a vector norm, commonly formulated as Euclidean  $L_2$ -norm. Based on how spatial contiguity is treated, regionalization algorithms may be classified into two main categories, spatially implicit methods and spatially explicit methods (Duque *et al.* 2007).

Spatially implicit methods first apply a generic clustering algorithm to the set of attribute vectors, without necessarily defining geographically connected regions. Post-processing steps are performed afterwards to impose spatial contiguity on each region. To achieve spatial contiguity, non-connected regions may be broken into connected parts (Openshaw and Wymer 1995). After that, manual refinement may be performed. Spatially implicit methods have several drawbacks. First, they do not allow a strict control of the resulting number of regions, as post-processing may produce a different number of regions than previously specified. Second, to impose a fixed number of output regions, manual refinement or domain knowledge may be required, which cannot be exempt of subjectivity (Aydin *et al.* 2021). Third, the shape of the regions is subject to the choice of the clustering algorithm (Duque *et al.* 2007). We hold that the first disadvantage is not critical if the number of regions is not strictly constrained. In geographical modelling, the number of regions is typically not known *a priori*. We extend a common approach (K-Means algorithm) and propose an automated post-processing procedure, which reduces subjectivity. The third issue is not addressed in our work. An extension of other clustering methods (e.g., hierarchical or density-based clustering) to our framework is not straightforward and would go beyond the scope of this study.

Spatially explicit methods consider spatial contiguity during the regionalization process, which ensures connectivity of regions without requiring post-processing operations. Duque *et al.* (2011) proposed three MIP formulations of this problem, which could be solved with commercial optimization software directly, and the optimal solution is guaranteed to be found. However, such exact methods are computationally expensive and therefore suitable to small datasets only. It would require more than three hours to solve a simulated case on a  $7 \times 7$  grid<sup>2</sup>.

While heuristic methods do not guarantee to find the optimal solution, their computational advantages make them more suitable for large datasets. Openshaw (1977) proposed the AZP algorithm, which uses an iterative process aiming at improving an initial solution by moving a unit from one region to another while ensuring spatial contiguity. This algorithm was improved by incorporating intelligent optimization techniques, such as simulated annealing and tabu search (Openshaw and Rao 1995). Assunção *et al.* (2006) proposed SKATER algorithm which operates by cutting edges from the minimum spanning tree. Inspired by hierarchical clustering algorithms, Guo (2008) proposed REDCAP algorithm, which supports single linkage, average linkage, and full linkage distances. The latter two algorithms may produce more accurate and stable results compared to AZP (Aydin *et al.* 2021). As a component of PySAL, a

---

<sup>2</sup>The experiments are performed using ILOG CPLEX 11.2 and executed on a computer with 8 GB of memory and a 2.99 GHz processor. See Duque *et al.* (2011) for further detail.

python spatial analysis library (Rey *et al.* 2021), Rey developed Regional-K-Means algorithm, which uses a workflow similar to K-Means, but it checks spatial contiguity before each move. We find that SKATER and REDCAP rely on similarity measures of attributes, thus a generalization to other modelling scenarios is not straightforward, while Regional-K-Means can be extended in a similar way with K-Means. AZP offers more flexibility on the objective function, which makes it adaptable to other modelling scenarios. Therefore, we consider AZP and Regional-K-Models in this study.

Statistical tests may provide a rigorous framework to assess heterogeneity between regions (spatially stratified heterogeneity). Wang *et al.* (2016) introduced q-statistic to assess the degree of statistical significance of spatially stratified heterogeneity. Yet this method considers heterogeneity of attribute values only. Adapting a similar method to geographical models aiming at making inference on processes would require further studies and is beyond the scope of this study.

An issue closely related to regionalization is the modifiable areal unit problem (MAUP). In the context of spatial data, analytical results, such as correlation and regression coefficients, may depend on the scale and configuration of areal units (Clark and Avery 1976, Fotheringham and Wong 1991). Openshaw (1977) argues that regionalization methods may solve this problem by optimizing the set of regions; yet the optimization criteria remain subjective (Fotheringham and Wong 1991). Regionalization methods also provide tools to investigate MAUP, in the sense that extreme cases could be constructed through optimization (Openshaw and Rao 1995).

### 3. Framework

#### 3.1. Geographical models

The geographical models considered in our framework can be viewed as a quantitative representation of spatial data or process, with regard to each spatial unit in a spatial domain discretized into a lattice<sup>3</sup>. Generally, geographic models aim at estimating parameters  $\hat{\theta}$  given a model  $\mathcal{M}$  with parameters  $\theta \in \Theta$ , a dataset  $D$ , and a discretized domain  $\mathcal{D}$ . The dataset  $D$  includes data measured in each spatial unit  $u_i$  within the domain  $\mathcal{D}$ . For example, in a linear regression model,  $D$  includes a dependent variable  $y_i$  and typically several features  $\mathbf{x}_i$  measured in each  $u_i$  within  $\mathcal{D}$ . The inference process may be expressed as follows (Equation 2):

$$\{D, \mathcal{M}(\theta), \mathcal{D}\} \longrightarrow \hat{\theta} \quad (\theta \in \Theta). \quad (2)$$

Our framework can accommodate a wide range of geographic models, which may be classified into three categories:

- (1) Attribute models that estimate the expected value (average) or range of plausible values in a region, with attributes only ( $D = \{\mathbf{y}\}$ ). For example, these models may estimate the annual mean precipitation or the range of plausible temperatures in a study area.
- (2) Regression models describing the relationship between features and an attribute ( $D = \{\mathbf{x}, \mathbf{y}\}$ ). For example, a linear regression model may describe the variation of gross domestic product (GDP) between countries based on two features: population size and number of enterprises.

---

<sup>3</sup>Note that we consider geographic models applied to lattice data only, which makes regionalization straightforward (aggregating polygons). Point process and network flow data are excluded from this study.

**Table 1.** Framework configuration in three typical modelling scenarios (columns 1-3)

Component	(1) Attribute models Attribute-based regionalization	(2) Regression models Regionalized regression	(3) Complex geographic models Interaction modelling
Data $D$	$\{y_i\}_{i=1}^N$	$\{(x_i, y_i)\}_{i=1}^N$	$\{G_i\}_{i=1}^N$
Model $\mathcal{M}$	$\mu \in \mathbb{R}^p$	$y = \beta \mathbf{x} + \alpha$	$g_{k,l} = cp_k^a p_l^b / d_{k,l}^\omega$
Error function $\epsilon$	$\ y_i - \mu\ _2^2$	$(\beta \mathbf{x}_i + \alpha - y_i)^2$	$\sum_{k,l} (h_{k,l} - cp_k^a p_l^b / d_{k,l}^\omega)^2$
Fitting method $f$	Mean	OLS	OLS or simulated annealing

- (3) Complex geographic models used to describe geographical processes within a spatial unit. Examples include spatial interaction models between places within a spatial unit, and cellular automata for land use change.

Examples for applying our framework to the three class of models are provided in Table 1. Attribute-based regionalization is the basic case considered by previous studies (Duque *et al.* 2007, 2011, Aydin *et al.* 2021) and can be solved with K-Means and Regional-K-Means algorithms. Regionalized regression models aim to delineate regions with homogeneous relationship between the independent variables  $\mathbf{x}$ , and the dependent variable  $y$ . A set of regression parameters  $\theta = \{\alpha, \beta\}$  will be estimated for each region. We further investigate this scenario in Section 4. Our framework is applicable to a variety of complex geographic models as well. As an example, we discuss the gravity model for spatial interactions in Section 5.

Note that we exclude models which are only applied to an entire region (composed of a set of spatial units), rather than considering each spatial unit in a region. For example, global auto-correlation statistics applied to spatial cross-sectional data generate a unique aggregated value computed for a region based on auto-correlation of attribute values between each spatial unit. For similar reasons, we do not consider spatial interaction models between units either. While qualitative models may be relevant in some cases, handling statements such as “the weather is hot” is not straightforward in an optimization setting. Future work using natural language processing models and fuzzy mathematics may investigate incorporating such statements.

### 3.2. Framework overview

Our framework aims at jointly estimate the regional parameters  $\theta$  of a geographic model  $\mathcal{M}$ , denoted as  $\theta = \{\theta_j\}_{j=1}^\gamma$ , along with the number of regions  $\gamma$  and the delineation of regions  $\mathcal{R} = \{\mathcal{R}_j\}_{j=1}^\gamma$  within a study domain  $\mathcal{D}$ . The input of the framework includes: a set of areal units  $\{u_i\}_{i=1}^N$ , a dataset  $D$  with values provided for each areal unit, and a geographic model  $\mathcal{M}$  with parameters  $\theta$  that are allowed to vary across the regions within the domain  $\mathcal{D}$ . During the optimization process, the spatial areal units  $\{u_i\}_{i=1}^N$  are aggregated into spatially connected regions  $\{\mathcal{R}_j\}_{j=1}^\gamma$ , so that optimal parameter values and regions are obtained. Note that  $D$  and  $\theta$  may represent various quantities according to different modelling settings. Within a simple linear regression model with a single feature, the dataset would include one dependent and one independent variable ( $D = \{(x_i, y_i)\}_{i=1}^N$ ) with parameters composed of an intercept and a feature coefficient that may vary across each region ( $\theta_j = \{\alpha_j, \beta_j\}$ ). The inference

Data	Model selection	Objective function	Optimization	Output
Spatial domain $\mathcal{D} = \{u_i\}_{i=1}^N$	Model $\mathcal{M}(\theta)$	$\mathcal{L} = \mathcal{E}(\mathbf{y}, \hat{\mathbf{y}}) + \lambda \mathcal{C}(\mathcal{R})$	<b>Spatially explicit</b> AZP Regional-K-Models	Regions $\mathcal{R} = \{\mathcal{R}_j\}_{j=1}^\gamma$
Dataset $D = \{(x_i, y_i)\}_{i=1}^N$	Fitting algorithm $f$	$\mathcal{E}$ : inductive error $\mathcal{C}$ : complexity $\mathcal{R}$ : the region scheme $\lambda$ : hyperparameter	<b>Spatially implicit</b> K-Models	Regional parameters $\theta = \{\theta_j\}_{j=1}^\gamma$

**Figure 1.** An overview of the proposed framework.

process of the suggested framework may be expressed as follows (Equation 3):

$$\{D, \mathcal{M}(\theta), \mathcal{D}\} \longrightarrow \{\mathcal{R}_j, \hat{\theta}_j\}_{j=1}^\gamma \quad (\theta_j \in \Theta). \quad (3)$$

Figure 1 provides an overview of the proposed framework. The analytical procedure includes three major steps: model selection, objective function definition, and optimization. In the model selection step, a model  $\mathcal{M}(\theta)$  is specified, together with a parameter space  $\Theta$ , which defines the possible values of the model parameters<sup>4</sup>. A corresponding fitting algorithm  $f$  is required, which is the calibration algorithm for  $\mathcal{M}(\theta)$  in the general case. It is used to estimate and update the regional parameters in the regionalization process. To combine both the model’s accuracy and ability to reconstruct the regions, we include two terms in the objective function: (a) an error term measuring the discrepancies between the model predictions and the observations and (b) a penalty term used to favor parsimonious models. We investigate and compare three available optimization algorithms to optimize the regionalization scheme, including two spatially explicit and one spatially implicit algorithms.

### 3.3. Objective function

In our framework, the determination of an optimal number  $\gamma$  and the delineation of regions are constrained to account for the trade-off between the accuracy and the generality of the model. Note that generality is obtained when a set of parameters is applied to a large area, rather than a specific location. While allowing the model parameters to vary for each spatial unit within a domain would maximize accuracy and potentially eliminate the model errors, each set of parameters would only be applicable to its corresponding spatial unit. On the other extreme, forcing the parameters to be invariant across the whole domain would maximize the model’s generality. Yet the latter would not be able to reveal potential heterogeneity between regions within the domain. Hence, jointly learning the optimal number of regions and their delineation while minimizing the model errors may lead to the identification of an optimal solution that accounts for both model accuracy and generality. In our framework, this is obtained by minimizing the following objective function (Equation 4):

$$\mathcal{L}(\mathcal{R}, \theta) = \mathcal{E}(\mathbf{y}, \hat{\mathbf{y}}) + \lambda \mathcal{C}(\mathcal{R}), \quad (4)$$

<sup>4</sup>In our framework, we specify a class of model from which parameters will be estimated. Note that for a given class of models, the number of parameters are allowed to vary according to dynamic changes in the number of regions during the optimization process.

where  $\mathcal{E}$  stands for inductive error, which is a function measuring the total error between the model predictions  $\hat{\mathbf{y}}$  and the observed data  $\mathbf{y}$ .  $\mathcal{C}$  stands for complexity, a function measuring the complexity of the regionalization scheme  $\mathcal{R} = \{\mathcal{R}_j\}_{j=1}^\gamma$ . We set  $\mathcal{C}(\mathcal{R}) = \gamma$  to penalize solutions proportionally to the number of output regions<sup>5</sup>. To allow different penalty levels associated with the complexity, we introduced the hyperparameter  $\lambda$ . A higher value of  $\lambda$  favors simpler solutions, and hence, tends to produce less regions. More specifically, the inductive error  $\mathcal{E}$  is the sum of the modelling errors  $\epsilon(\cdot)$  computed in each spatial unit  $u_i$ , with  $i = 1, \dots, N$  (Equation 5):

$$\mathcal{E}(\mathbf{y}, \hat{\mathbf{y}}) = \sum_{i=1}^N \sum_{j=1}^{\gamma} I[u_i \in \mathcal{R}_j] \epsilon(\hat{y}_{i,j}, y_i), \quad (5)$$

where  $y_i$  is data<sup>6</sup> observed at  $u_i$ ;  $\hat{y}_{i,j}$  is the model prediction at  $u_i$  with parameters  $\theta_j$ ;  $I[\text{cond}]$  is an indicator function, which takes value 1 if the condition (cond) is true and 0 otherwise. The function  $\epsilon$  measures the local modelling error in a spatial unit. A fitting algorithm  $f$  is used to estimate the model parameters  $\hat{\theta}_j$  used in region  $\mathcal{R}_j$ , which can be expressed as follows (Equation 6):

$$\hat{\theta}_j = \arg \min_{\theta_j \in \Theta} \sum_{i=1}^N I[u_i \in \mathcal{R}_j] \epsilon(\hat{y}_{i,j}, y_i). \quad (6)$$

In attribute-based regionalization, we have  $\epsilon(\hat{y}_{i,j}, y_i) = \|y_i - \mu_j\|^2$ . The form of the error  $\mathcal{E}$  is the same with the objective function in generic clustering analysis<sup>7</sup>. The mean vector of attributes

$$\mu_j = \frac{1}{|\mathcal{R}_j|} \sum_{i=1}^N I[u_i \in \mathcal{R}_j] y_i \quad (7)$$

is the exact solution of Equation 6. In the case of regionalized regression, the linear models are calibrated through ordinary least squares estimation (OLS), which minimizes the sum of squared errors (SSE).

### 3.4. Optimization algorithms

We compare the performance of three algorithms to optimize the objective function and reconstruct the regions. This includes two spatially explicit algorithms, AZP and Regional-K-Models, and one spatially implicit algorithm, K-Models (with post-processing). All considered algorithms start with an initial feasible solution and execute an iterative process to find an optimal solution. In K-Models and Regional-K-Models,

<sup>5</sup>Our framework could have incorporated other complexity elements such as perimeter or compactness of regions. However, to make our framework as general as possible, we favored a simple formulation for region complexity, i.e. the number of regions, which can be applicable in all considered geographical models without additional adjustments.

<sup>6</sup>Note that the observed data  $x_i$  and  $y_i$  associated with  $u_i$  can be vectors rather than scalars. We describe the scalar case to simplify the notation. Generalizing the equations and algorithms to vector objects is straightforward.

<sup>7</sup>Note that in Equation 1, the number of considered unit pairs in the sum is  $\sum_{j=1}^M \binom{|R_j|}{2}$ , which is smaller if  $|R_j| (j = 1, \dots, M)$  are close to each other. Hence that objective function might favor solutions whose regions have similar numbers of units, while the objective function defined here does not suffer from this issue.



---

**Algorithm 1** K-Models

---

**Input:** Domain  $\mathcal{D}$  composed of spatial units  $\{u_i\}_{i=1}^N$ ; data  $D = \{(x_i, y_i)\}_{i=1}^N$ ; number of regions  $K$ ; maximum iterations  $L$ .

**Output:** Regions  $\{\mathcal{R}_j\}_{j=1}^K$  and estimated parameters  $\{\hat{\theta}_j\}_{j=1}^K$ .

- 1: Generate initial regions  $\{\mathcal{R}_j\}_{j=1}^K$  and estimate initial parameters  $\{\hat{\theta}_j\}_{j=1}^K$ ;
  - 2: stable = False;
  - 3:  $t = 0$ ;
  - 4: **while** not stable and  $t < L$  **do**
  - 5:    $\mathcal{R}'_j = \emptyset, j = 1, 2, \dots, K$ ;
  - 6:   **for**  $i = 1, 2, \dots, N$  **do**
  - 7:     Identify the region whose parameters fit  $(x_i, y_i)$  best:  $r_i = \arg \min_j \epsilon(y_i, \hat{y}_{i,j})$ ;
  - 8:     Add  $u_i$  to the region with the lowest error at  $u_i$ :  $\mathcal{R}'_{r_i} = \mathcal{R}'_{r_i} \cup \{u_i\}$ .
  - 9:   **for**  $j = 1, 2, \dots, K$  **do**
  - 10:     Estimate the model parameters:  $\hat{\theta}'_j = \arg \min_{\theta_j \in \Theta} \sum_{i=1}^N I[u_i \in \mathcal{R}'_j] \epsilon(y_i, \hat{y}_{i,j})$ ;
  - 11:   **if**  $\mathcal{R}_j = \mathcal{R}'_j$ , with  $j = 1, 2, \dots, K$  **then**
  - 12:     stable = True
  - 13:   Update regions and parameters:  $(\mathcal{R}_j, \hat{\theta}_j) = (\mathcal{R}'_j, \hat{\theta}'_j)$ , with  $j = 1, 2, \dots, K$ ;
  - 14:    $t = t + 1$ ;
  - 15: **return**  $\{\mathcal{R}_j, \hat{\theta}_j\}_{j=1}^K$ .
- 

a unit can only be moved into the region with the “closest” model (i.e. the model with the least residual). However, in AZP, a move is allowed as long as it decreases the value of the objective function.

### 3.4.1. K-Models with post-processing

We introduce K-Models as an extension of the classical K-Means clustering algorithm (MacQueen 1967). In the K-Models algorithm, we associate each region with a set of model parameters, which takes the role of cluster centers in K-Means. A cluster center is described by the mean vector, a set of model parameters in  $\mathbb{R}^p$ , where  $p$  is the number of features. Thus, K-Means is a special case of K-Models.

The K-Models algorithm starts with a randomly generated initial regionalization scheme with  $K$  regions, which satisfies the spatial contiguity constraint. For each initial region  $\mathcal{R}_j$ , a set of model parameters  $\theta_j$  is initialized using the fitting algorithm  $f$ . Each iteration includes two steps. First, for each spatial unit, the error of each regional model is calculated, and the unit is moved to the region whose model fits it best. Second, the model parameters of each region are updated with  $f$ , as units are moved into or out of the region in the first step. The algorithm stops if no unit is moved during an iteration, or when the maximum number of iterations is reached. Note that the objective function value is non-increasing in both steps. The pseudo code for this algorithm is provided in Algorithm 1.

To generate the initial solution,  $K$  random seeds are picked from  $\{u_i\}_{i=1}^N$ . Next, for each region, if it has unassigned neighboring units, one of them is randomly chosen and moved into the region. This procedure is repeated until every unit is assigned into a region. This method ensures the spatial contiguity of each region. The resulting regions from the K-Models procedure are not necessarily connected. A post-processing

procedure is introduced to ensure the connectivity of each region, as well as improve the solution. First, if a region is disconnected, it is divided into connected branches. A new set of model parameters is fitted for each branch. After this step, the number of regions may be larger than  $K$ . Second, we examine each pair of neighboring regions, and calculate changes in the objective function if they are merged (a new set of model parameters is fitted for the merged region). The pair of regions that produces the largest decrease of the objective function value are merged into one region. This procedure is repeated until no additional decrease in the objective function value can be obtained by merging two neighboring regions. The idea of merging after partitioning is similar with two-stage clustering algorithms such as Chameleon (Karypis 1999).

Similar with K-Means, a parameter  $K$  is required as input. However, due to the merging procedure, it is  $\lambda$  that largely determines the number of regions produced, not  $K$ . As long as  $K$  is not too small, the algorithm is able to produce regions with reasonable sizes. One can further improve the identification of the lowest objective value by exploring different values of  $K$ . In rare cases, the K-Models algorithm may produce an empty region in the process. Such cases are more frequent if  $N \gg K$  does not hold. A simple remedy to this issue is to delete the empty region, as the parameter  $K$  does not actually restrict the final estimated number of output regions.

### 3.4.2. AZP

Of the three algorithms, AZP is the most flexible in terms of the form of the objective function. If the function  $\mathcal{E}(\mathbf{y}, \hat{\mathbf{y}})$  is not in the form of Equation 5, AZP is still applicable, while the other two algorithms based on K-Means are not. Using the same method applied in K-Models, an initial solution is generated, which satisfies the spatial contiguity constraint. Subsequently, AZP tries to improve the solution by moving a region’s neighboring unit into the region. A unit is neighbor of a region if their boundary share a common edge. The AZP procedure is described in Algorithm 2.

Two conditions need to be met to allow moving a unit from one region to another: (a) the donor region remains connected after giving out the unit; (b) the move leads to a decrease in the objective function value. The first condition involves the verification of graph connectivity. A breadth-first search approach has a time complexity of  $O(|E|)$ , where  $E$  is the set of edges in the adjacent graph. Assessing the validity of the second condition for spatial unit  $v$  in the neighborhood of  $\mathcal{R}_j$  requires fitting new models for  $\mathcal{R}_j \cup \{v\}$  and  $\mathcal{R}_d \setminus \{v\}$ . For attribute models such as mean vectors, the time complexity is  $O(N)$ . Yet it would require much more operations to fit the models in a linear regression setting. Therefore, the less computationally expensive condition should be verified first, which depends on the modelling scenario. In the presence of two or more valid neighboring units of  $\mathcal{R}_j$ , only one unit is moved, as it may affect the validity of subsequent moves. Figure 2a illustrates the potential issues associated with simultaneous moves.

Unless an empty region is produced during the process, the output of AZP consists of exactly  $K$  regions. In other words, if  $\mathcal{C}(\mathcal{R}) = \gamma$ , the parameter  $\lambda$  does not play a role during the process. Hence, it is necessary to search different  $K$  values to identify the best solution (Equation 4).

### 3.4.3. Regional-K-Models

We propose to extend Regional-K-Means algorithm (Feng *et al.* 2021), which is further referred to as Regional-K-Models. In contrast to the K-Models algorithm, spatial

---

**Algorithm 2** AZP

---

**Input:** Domain  $\mathcal{D}$  composed of spatial units  $\{u_i\}_{i=1}^N$ ; data  $D = \{(x_i, y_i)\}_{i=1}^N$ ; number of regions  $K$ .

**Output:** Regions  $\{\mathcal{R}_j\}_{j=1}^K$  and estimated parameters  $\{\hat{\theta}_j\}_{j=1}^K$ .

- 1: Generate initial regions  $\{\mathcal{R}_j\}_{j=1}^K$  and estimate initial parameters  $\{\hat{\theta}_j\}_{j=1}^K$ ;
  - 2: stable = False;
  - 3: **while** not stable **do**
  - 4:     stable = True;
  - 5:     **for**  $j = 1, 2, \dots, K$  **do**
  - 6:          $P = \emptyset$ ;
  - 7:         **for**  $v$  in the set of units which are connected with  $\mathcal{R}_j$  **do**
  - 8:             Find the region  $\mathcal{R}_d$  such that  $v \in \mathcal{R}_d$ ;
  - 9:             **if**  $\mathcal{R}_d \setminus \{v\}$  is connected and moving  $v$  to  $\mathcal{R}_j$  decreases the value of the objective function **then**
  - 10:                  $P = P \cup \{v\}$ ;
  - 11:             **if**  $P \neq \emptyset$  **then**
  - 12:                 stable = False;
  - 13:                 Randomly choose  $v \in P$ ;
  - 14:                 Move  $v$  into  $\mathcal{R}_j$ , and update the model parameters.
  - 15: **return**  $\{\mathcal{R}_j, \theta_j\}_{j=1}^K$ .
- 

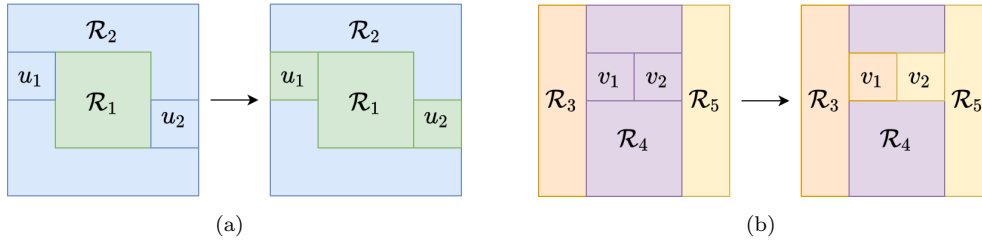


**Figure 2.** Examples of spatial contiguity breaks that may occur if two moves are performed simultaneously. (a)  $\mathcal{R}_1, \mathcal{R}_2$  are regions, and units  $u_1, u_2$  initially belong to  $\mathcal{R}_2$ . In AZP algorithm, moving  $u_1$  or  $u_2$  into  $\mathcal{R}_1$  satisfies the contiguity constraint, while moving both of them into  $\mathcal{R}_1$  simultaneously makes  $\mathcal{R}_2$  disconnected. (b) In Regional-K-Models, a similar situation may occur for region  $\mathcal{R}_4$ , if  $v_1$  is moved into region  $\mathcal{R}_3$ , and simultaneously,  $v_2$  is moved into  $\mathcal{R}_5$ , although either move is in principle valid.

contiguity is checked before each move, which makes Regional-K-Models spatially explicit. The procedure of Regional-K-Models is described in Algorithm 3. Similar with K-Models, the objective function is non-increasing in both unit moving and model updating.

As a unit is allowed to be moved into its neighboring region with the best model fit only, the range of potential candidate moves is rather restricted compared with AZP. Similar to AZP, only one candidate move is performed at a time to prevent potential break of the contiguity constraint induced by simultaneous moves (see illustrated example in Figure 2b) and different values of  $K$  are investigated to find the optimal solution.

---

**Algorithm 3** Regional-K-Models

---

**Input:** Domain  $\mathcal{D}$  composed of spatial units  $\{u_i\}_{i=1}^N$ ; data  $D = \{(x_i, y_i)\}_{i=1}^N$ ; number of regions  $K$ .

**Output:** Regions  $\{\mathcal{R}_j\}_{j=1}^K$  and estimated parameters  $\{\hat{\theta}_j\}_{j=1}^K$ .

```
1: Generate initial regions  $\{\mathcal{R}_j\}_{j=1}^K$  and estimate initial parameters  $\{\hat{\theta}_j\}_{j=1}^K$ ;
2: stable = False;
3: while not stable do
4:   stable = True;
5:    $P = \emptyset$ ;
6:   for  $i = 1, 2, \dots, N$  do
7:     Identify the region  $\mathcal{R}_{d_i}$  that contains  $u_i$ ;
8:     Identify the region  $\mathcal{R}_{r_i}$  with the lowest local error:  $r_i = \arg \min_j \epsilon(y_i, \hat{y}_{i,j})$ ;
9:     if  $d_i \neq r_i$  and  $\mathcal{R}_{d_i} \setminus \{u_i\}$  and  $\mathcal{R}_{r_i} \cup \{u_i\}$  is connected then
10:        $P = P \cup \{u_i\}$ ;
11:   if  $P \neq \emptyset$  then
12:     stable = False;
13:     Randomly choose  $u_i \in P$ ;
14:     Move  $u_i$  into  $\mathcal{R}_{r_i}$ , and update the related model parameters.
15: return  $\{\mathcal{R}_j, \theta_j\}_{j=1}^K$ .
```

---

#### 4. Application in spatial regression scenarios

To assess the validity and usefulness of the proposed regionalization framework, we performed a set of experiments within a spatial regression context. Spatial regression models allow identifying and quantifying effects of features on a response, while accounting for spatial dependency in the data, and making spatial predictions. Spatial lag models (SLM, Anselin (2010)) and geographically weighted regression (GWR, Brunson *et al.* (1996)) are two common approaches. SLM is a family of global regression models which incorporate spatial lag effects to account for spatial dependency within a neighborhood. GWR is a local regression approach, modelling spatial heterogeneity by allowing parameters to vary across space. Our approach is complementary to SLM and GWR, by including a regionalization process and a spatial regression model that is calibrated for each region. We term it *regionalized regression*, which is at the midpoint between global regression and local regression. It is a spatial variant of multilevel linear regression (Gelman and Hill 2007), where data are divided into groups, and coefficients are allowed to vary for different groups. In regionalized regression, each group stands for a geographically connected region.

Note that regionalized regression can be performed using the framework of GWR as well. For each spatial unit, GWR estimates a set of linear regression coefficients. Thus, an attribute-based regionalization can be applied to the estimated local coefficients, and produce connected regions with a similar relationship between variables. In this GWR approach, the estimation of the regression coefficients and region delineation are optimized separately. As a complementary approach, the proposed framework jointly optimizes region delineation along with the estimation of the regression coefficients, which can lead to optimal solutions maximizing the overall model accuracy while minimizing the number of regions.

We performed linear regression experiments on two synthetic datasets, as well as real data gathered from the Georgia open dataset (Yu *et al.* 2020). We implement

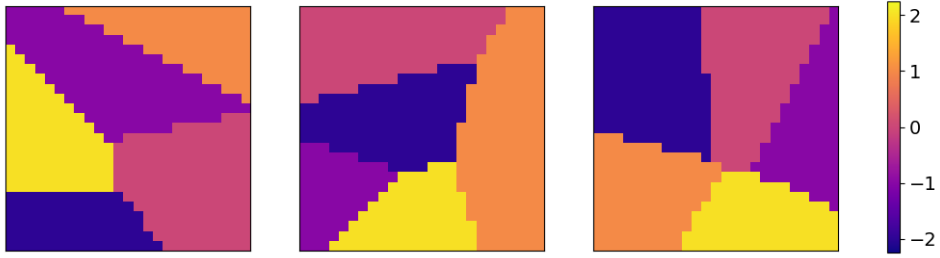


**Figure 3.** Three examples of the parameter surface of  $\beta_1$  in Dataset 1. In each simulation, the parameter surface is generated by Voronoi polygons of five random seed points. Each polygon is assigned a different value of  $\beta_1$ .

and test all three algorithms of our framework and included the GWR method as benchmark.

#### 4.1. *Simulation design*

Simulated data experiments are performed on a  $25 \times 25$  grid, where each grid cell represents a spatial unit. For each cell, each independent variable  $x_i$  is generated from an independent uniform distribution in  $[0, 1)$ ; the dependent variable  $y$  is generated from a linear model, with predefined linear coefficients. Rook contiguity (cells sharing a side are considered neighbors) is used in all simulations. We simulate two datasets (Dataset 1 and Dataset 2).

In Dataset 1, the relationship between  $x$  and  $y$  exhibits a strict stratified heterogeneity. That is, the linear coefficients are identical in each predefined region, and distinct in different regions. This simulation aims to test whether our framework can reconstruct the underlying regions associated with geographical processes, given the spatial distributions of  $x$  and  $y$ . The data generating process can be expressed as follows (Equation 8):

$$y = \beta_0 + \beta_1 x + \epsilon, \quad \epsilon \sim \mathcal{N}(0, \sigma^2) \quad (8)$$

where  $x \sim \mathcal{U}[0, 1)$ ,  $\beta_0 \equiv 0$ , and the errors follow a normal distribution with mean 0 and variance  $\sigma^2$ . Five cells are randomly picked as seed points, and their corresponding Voronoi polygons produce five spatially connected regions  $\mathcal{R}_1, \dots, \mathcal{R}_5$ . The covariate coefficient  $\beta_1$  are set as -2, -1, 0, 1, 2 in region  $\mathcal{R}_1, \dots$ , and  $\mathcal{R}_5$ , respectively (Figure 3).

In Dataset 2, the relationship between  $\mathbf{x}$  and  $y$  varies continuously across space. This dataset mimics a real case scenario that is common in environmental sciences, where the change in model parameters is gradual across region boundaries, instead of the abrupt changes between regions in Dataset 1. The data generating process of Dataset 2 can be expressed as follows (Equation 9):

$$y = \beta_0 + \beta_1 x_1 + \beta_2 x_2 + \epsilon, \quad \epsilon \sim \mathcal{N}(0, \sigma^2) \quad (9)$$

where  $x_1, x_2 \sim \mathcal{U}[0, 1)$ . The linear coefficients are set to express distinct levels of

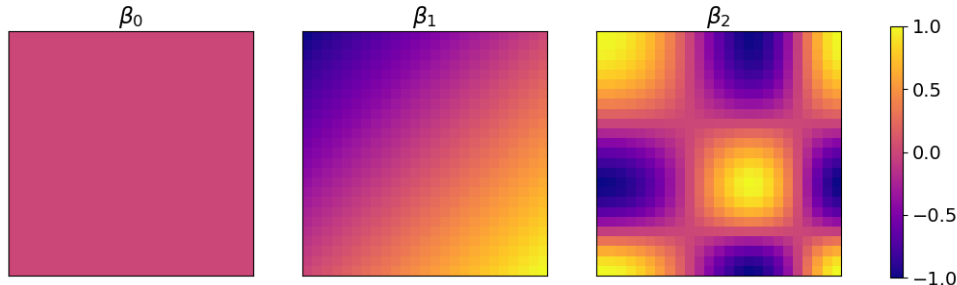


**Figure 4.** Parameter surfaces in Dataset 2.  $\beta_0$  is constant over space.  $\beta_1$  is a slope from bottom right to top left.  $\beta_2$  is highly vibrated with several peaks and valleys. The three parameters represent distinct levels of spatial heterogeneity.

heterogeneity (Fotheringham *et al.* 2017),

$$\beta_0 = 0 \tag{10}$$

$$\beta_1 = \frac{1}{24}(r + c) - 1 \tag{11}$$

$$\beta_2 = \cos(\pi e^{r/22}) \cos(\pi e^{c/22}) \tag{12}$$

where  $r, c$  are row and column numbers in the grid (from 0 to 24), respectively. The parameter surfaces are illustrated in Figure 4. In this setting,  $\beta_0$  is constant across space, with no heterogeneity.  $\beta_1$  has a non-zero slope that varies across space, with a maximum of 1 and a minimum of -1 at two opposite corners of the study domain.  $\beta_2$  shows a high level of heterogeneity, with five high value areas (peaks) and four low value areas (valleys). The variability of the sizes of peaks and valleys are designed to assess the ability of our approach to reconstruct regions of different sizes driven by heterogeneous processes with spatially varying scales (Fotheringham and Sachdeva 2022).

Using the data generating processes defined above, we produced a set of samples for both datasets. For Dataset 1, we set different values of  $\sigma$  to evaluate the effect of random noise on regionalization. Three conditions are considered, namely low noise ( $\sigma = 0.1$ ), medium noise ( $\sigma = 0.2$ ), and high noise ( $\sigma = 0.3$ ). 50 parameter surfaces are simulated, and three  $x, y$  arrays are generated for each parameter surface, using different noise levels.  $\lambda = 5$  is used for Dataset 1. For Dataset 2, with the parameter surfaces defined above, 50 sets of  $\mathbf{x}, y$  arrays are simulated. We test the cases where  $\lambda = 5$  and  $\lambda = 3$ , representing different regionalization scales. We assume low noise ( $\sigma = 0.1$ )<sup>8</sup>.

In this study we consider model complexity as the number of output regions. We run each algorithm with parameter  $K$  that varies from 2 to 20, and select the results that show the lowest objective function value<sup>9</sup>. For GWR, the derived local coefficients are regionalized with K-Means (the basic case of K-Models) and post-processing, as

<sup>8</sup>We consider different noise conditions only in the experiments carried out on Dataset 1. Obtaining distinct latent regions ease the assessment of regionalization performance.

<sup>9</sup>For GWR, we considered a larger range of  $K$  (2 to 60) since it appears to produce better results with values of  $K > 20$ .

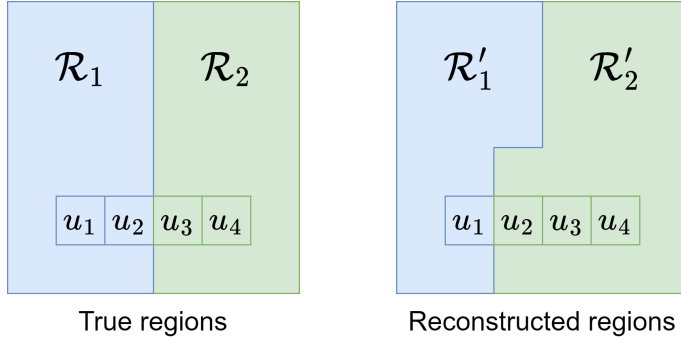


**Figure 5.** Four possible situations for a pair of spatial units in the calculation of Rand index.  $\mathcal{R}_1, \mathcal{R}_2$  are true regions,  $\mathcal{R}'_1, \mathcal{R}'_2$  are reconstructed regions,  $u_i (i = 1, 2, 3, 4)$  are units.  $(u_3, u_4)$  is a true positive (TP) pair,  $(u_1, u_2)$  is a false negative (FN) pair,  $(u_2, u_3), (u_2, u_4)$  are two false positive (FP) pairs,  $(u_1, u_3), (u_1, u_4)$  are two true negative (TN) pairs.

described in Section 3.4.1<sup>10</sup>. GWR applies an adaptive bisquare kernel with corrected Akaike information criterion (AICc) used as criterion to select the bandwidth (Fotheringham *et al.* 2017).

To compare the optimization performance of the considered algorithms, we report the objective function values. To assess the ability of the algorithms to reconstruct the latent regions, we compute the Rand index (RI) and the normalized mutual information (NMI) for experiments on Dataset 1. Such metrics are not applicable for Dataset 2 since there are no distinct underlying regions. We visually compare the delineated regions with latent parameter surfaces and check if the algorithms produce reasonable results.

To compare the true underlying regions and the reconstructed regions, we compute RI, which calculates the proportion of correctly grouped pairs of units (Rand 1971). There are four possible situations for each pair of spatial units, which are illustrated in Figure 5 with examples:

- True positive (TP): the two units are in the same region for both the true region scheme and the reconstructed region scheme.
- False negative (FN): the two units are in the same region in the true result, but mistakenly grouped into different regions by the algorithm.
- False positive (FP): the two units are in different regions in the true result, but mistakenly grouped into the same region by the algorithm.
- True negative (TN): the two units are in different regions for both the true region scheme and the reconstructed region scheme.

Rand index is calculated with the counts of the four types of pairs (Equation 13):

$$\text{RI} = \frac{TP + TN}{TP + FN + FP + TN}. \quad (13)$$

The possible range of Rand index is  $[0,1]$ . High values indicate a better region reconstruction. RI takes the maximal value of 1 if all reconstructed regions are identical to the true regions. NMI measures the difference of two region schemes from an information theory perspective (Vinh *et al.* 2010). Assume  $\mathcal{R} = \{\mathcal{R}_j\}_{j=1}^M$  are the true

<sup>10</sup>Note that GWR can be combined with other attribute-based regionalization algorithms such as AZP, SKATER and REDCAP. We use K-Means here to compare the results with the K-Models approach.

underlying regions, and  $\mathcal{R}' = \{\mathcal{R}'_j\}_{j=1}^\gamma$  are reconstructed regions. The entropy  $H(\mathcal{R})$  is defined as follows (Equation 14):

$$H(\mathcal{R}) = - \sum_{j=1}^M \frac{|\mathcal{R}_j|}{N} \log \frac{|\mathcal{R}_j|}{N}, \quad (14)$$

where  $N$  is the total number of units. The mutual information ( $I(\mathcal{R}, \mathcal{R}')$ ) of  $\mathcal{R}$  and  $\mathcal{R}'$  is defined as follows (Equation 15):

$$I(\mathcal{R}, \mathcal{R}') = \sum_{j=1}^M \sum_{k=1}^\gamma \frac{|\mathcal{R}_j \cap \mathcal{R}'_k|}{N} \log \frac{N|\mathcal{R}_j \cap \mathcal{R}'_k|}{|\mathcal{R}_j||\mathcal{R}'_k|}. \quad (15)$$

Based on the concepts above, NMI can be expressed as follows (Equation 16):

$$\text{NMI}(\mathcal{R}, \mathcal{R}') = \frac{I(\mathcal{R}, \mathcal{R}')}{H(\mathcal{R})H(\mathcal{R}')}. \quad (16)$$

The range of NMI is  $[0,1]$ . High NMI values indicate that one region scheme provides a large amount of information for the other, which suggests similarity between the two region schemes.

All experiments are performed on a computer with dual Intel Xeon Gold 5118 CPUs (2.30GHz) and 256GB of memory. The data generating process and regionalization algorithms are implemented in Python 3.9, utilizing the NumPy package (Harris *et al.* 2020). We use the linear regression API provided by scikit-learn (Pedregosa *et al.* 2011). Libpysal and mgwr (Oshan *et al.* 2019) modules in PySAL (Rey *et al.* 2021) are used as well for handling spatial weights and performing GWR, respectively.

## 4.2. Results

Table 2 shows the mean objective function values of the four algorithms associated with Dataset 1 and Dataset 2. For Dataset 1, the spatially implicit method, K-Models, shows a relatively good overall performance compared to the two spatially explicit methods, AZP and Regional-K-Models. K-Models achieves the best performance in all 150 test cases (50 simulations, each with three noise levels). As for GWR combined with K-Means, which is also a spatial implicit approach, it outperforms AZP and Regional-K-Models as well, yet shows a lower performance compared to K-Models. Table 3 shows the mean Rand index and NMI values for 50 simulations in Dataset 1. For all algorithms, both Rand index and NMI decreases as the noise level increases. K-Models achieves the best result for both metrics, regardless of the noise level. Regarding region reconstruction, the performance of AZP and Regional-K-Models is still not as good as GWR.

Figure 6 illustrates the regionalization results of a simulation from Dataset 1. Both K-Models and GWR were able to reconstruct relatively well the spatial distribution of the parameter values. As the noise level increases, the regionalization results show a slight discrepancy at the region boundaries, yet the general pattern remains correctly reconstructed. Results show that AZP and Regional-K-Models tend to produce regions with more branches, which are deviations from the true parameter surface. This



**Table 2.** Mean objective values obtained from 50 simulations on two simulated datasets.

Algorithm	Dataset 1			Dataset 2	
	Low noise	Medium noise	High noise	$\lambda = 5$	$\lambda = 3$
K-Models	<b>31.05</b>	<b>49.42</b>	<b>79.32</b>	<b>50.25</b>	<b>40.10</b>
AZP	59.60	87.26	120.10	58.14	48.89
Regional-K-Models	83.23	125.53	161.78	62.95	56.73
GWR	41.73	60.18	89.48	51.34	41.97

Noise levels stand for variance of the error term in the linear model. Low noise:  $\sigma = 0.1$ ; medium noise:  $\sigma = 0.2$ ; high noise:  $\sigma = 0.3$ . We set  $\lambda = 5$  for Dataset 1, and  $\sigma = 0.1$  for Dataset 2. The lowest objective function value in each simulation setting is put in bold.

**Table 3.** Mean values of Rand index (R) and normalized mutual information (NMI) obtained from 50 simulations on Dataset 1.

Algorithm	Low noise		Medium noise		High Noise	
	RI	NMI	RI	NMI	RI	NMI
K-Models	<b>0.9891</b>	<b>0.9551</b>	<b>0.9757</b>	<b>0.9128</b>	<b>0.9616</b>	<b>0.8728</b>
AZP	0.8715	0.7361	0.8399	0.6578	0.8211	0.6095
Regional-K-Models	0.8559	0.6784	0.8079	0.5752	0.8011	0.5569
GWR	0.9676	0.8802	0.9620	0.8644	0.9538	0.8399

In each simulation setting, the highest RI and NMI values are put in bold. Low noise:  $\sigma = 0.1$ ; medium noise:  $\sigma = 0.2$ ; high noise:  $\sigma = 0.3$ .

suggests that spatially explicit methods may have a disadvantage in regionalized regression. In spatially explicit methods, the options to improve the results are restricted by the contiguity constraint, which may lead to a sub-optimal result. Moreover, both algorithms seem to be affected by large random noise in the linear model.

For Dataset 2, the performance rank of the four algorithms, measured by the objective function, is similar to the results on Dataset 1. K-Models achieves the best result in 76% of the simulations (38 out of 50) when  $\lambda = 5$ , and in 92% of the simulations (46 out of 50) when  $\lambda = 3$ . GWR performs best in all but one of the remaining simulations. K-Models shows the best overall result, yet the improvement compared to GWR is marginal. Spatial explicit approaches, AZP and Regional-K-Models show a lower overall performance. Figure 7 shows the regionalization results of an illustrative simulation for  $\lambda = 5$  and  $\lambda = 3$ . The reconstructed regions appear jointly affected by the spatial variation of the coefficients  $\beta_1$  and  $\beta_2$ . All algorithms tend to delineate less regions in the case when  $\lambda = 5$ , as a large  $\lambda$  value corresponds to a higher penalty associated with the number of regions. K-Models and GWR seem to generate sensible results, reflected by an increase in  $\beta_1$  from the top left to the bottom right of the domain. Furthermore, they reconstruct larger peaks and valleys while ignoring smaller ones, which improves generality. AZP and Regional-K-Models generate undesirable branches. Moreover, Regional-K-Models often produces solutions with only two or three regions, indicating that the algorithm fails to find a better result for larger  $K$  values. This might be due to more limited candidate moves in Regional-K-Models compared to AZP.

The results demonstrate the ability of the proposed framework to discover latent homogeneous regions related to geographical processes. In the spatial regression scenario, the K-Models algorithm shows the best performance, outperforming the baseline method of GWR with attribute-based regionalization, as well as two spatially explicit methods. The processes involved in the algorithms include some degree of randomness. A different region initialization may affect the optimization result. The order in which

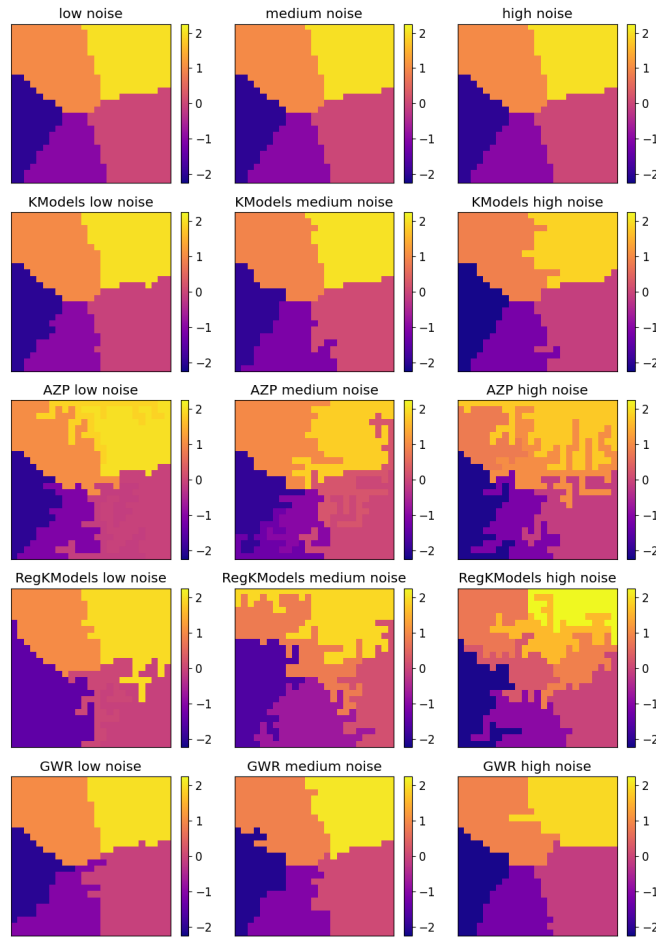


**Figure 6.** Regionalization results of one illustrative simulation in Dataset 1. The first row shows the true parameter surface of  $\beta_1$ . Cells in each region have the same coefficient value. Other rows show the estimated spatial distributions of  $\beta_1$  from four algorithms (K-Models, AZP, Regional-K-Models, and GWR). The columns show noise levels used in different experiments. Low noise:  $\sigma = 0.1$ ; medium noise:  $\sigma = 0.2$ ; high noise:  $\sigma = 0.3$ .

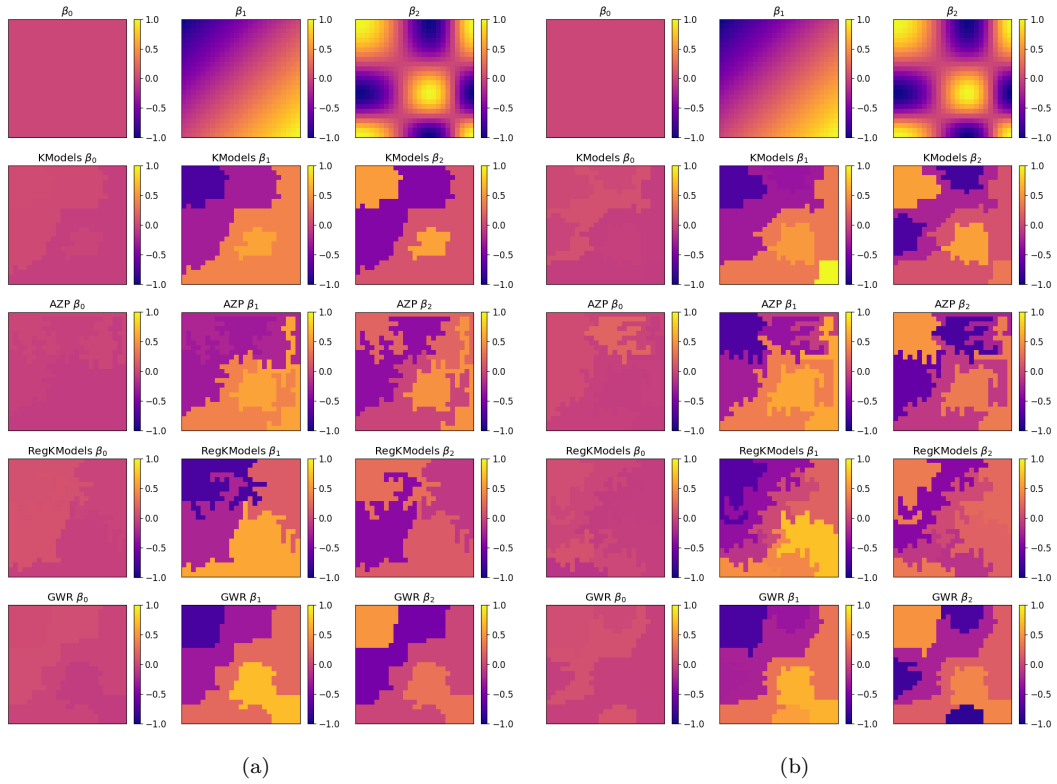


**Figure 7.** Regionalization results of one illustrative simulation in Dataset 2. The first row shows the true parameter surface of  $\beta_0, \beta_1, \beta_2$ , respectively. Other rows show the estimated spatial distributions of the parameters from four algorithms (K-Models, AZP, Regional-K-Models, and GWR). Each panel shows different values of  $\lambda$ , with (a)  $\lambda = 5$ ; (b)  $\lambda = 3$ .

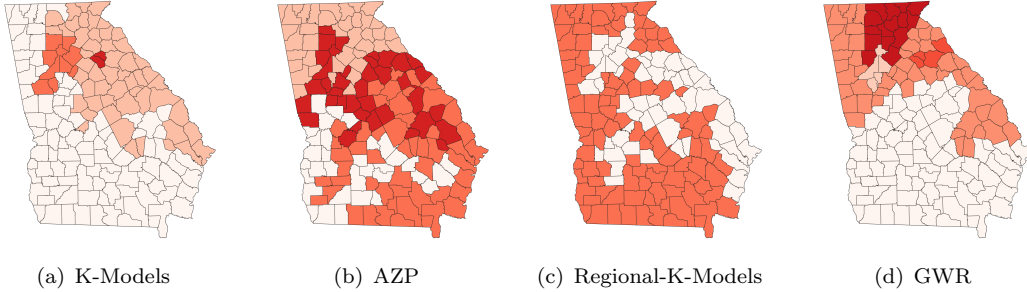


**Figure 8.** Regionalization results of the Georgia dataset. Each color represents a reconstructed region. We report the best solution among 10 repeating runs, along with the values of the objective function  $\mathcal{L}_{\text{algo}}$  for different algorithms (algo). (a) K-Models, 4 regions,  $\mathcal{L}_{\text{KM}} = 35.96$ ; (b) AZP, 4 regions,  $\mathcal{L}_{\text{AZP}} = 38.87$ ; (c) Regional-K-Models, 2 regions,  $\mathcal{L}_{\text{RKM}} = 43.78$ ; (d) GWR, 5 regions,  $\mathcal{L}_{\text{GWR}} = 38.69$ .

algorithms execute checks throughout all regions or units may lead to different reconstructed regions for the same dataset. In practice, repeated runs could be performed to identify more systematically the best optimization result. It requires about ten minutes to half an hour on our machine to regionalize a  $25 \times 25$  grid in the experiment above. We provide detailed results on the algorithm stability and running time in Appendix A. Appendix B provides further discussion on the choice of the hyperparameter  $\lambda$  and the effect of changes in  $K$  values.

### 4.3. An empirical example

We performed regionalized regression on the Georgia open dataset, a sample dataset from the mgwr software (Oshan *et al.* 2019). This dataset has been used in previous spatial regression studies (e.g., Fotheringham *et al.* (2002), Griffith (2008), Yu *et al.* (2020)). The data are collected from a population census in 1990 and include socio-economic attributes of 159 counties in Georgia, USA (Oshan *et al.* 2019). We consider the regression of the percentage of people with a bachelor’s degree or higher (PctBach), with intercept and explanatory variables including the percentage of people born in a foreign country (PctFB), the percentage of African American (PctBlack), and the percentage of rural residents (PctRural). To ease comparison of the results with those from GWR, we use the same explanatory variables as in Yu *et al.* (2020).

We compare the three algorithms from the proposed framework, as well as GWR. We set  $\mathcal{C}(\mathcal{R}) = \gamma$ , with  $\gamma$  the number of output regions and  $\lambda = 3$ . We search a set of  $K$  values identical to those used in the experiments on simulated data above. Each algorithm is repeated 10 times to obtain better optimization results. The results show that K-Models achieves the lowest objective function value, followed by GWR and AZP (Figure 8)<sup>11</sup>. We observe that all three algorithms show a general discrepancy along the north-south axis. The overall performance of Regional-K-Models is mediocre, as illustrated by the highest objective function value obtained among the four algorithms.

We focus on the result of the K-Models algorithm, which is the best solution according to the objective function values. Figure 9 shows the estimated coefficients on standardized data for each region. We observe an outlier region with only 2 units (counties), where the number of units is less than the number of linear coefficients. In this case, the algorithm uses the minimal-norm solution of normal equations in

<sup>11</sup>Note that predicted percentages should be within 0 and 100%. All local predictions of the four results were within this range, so no truncation was needed in the experiments.

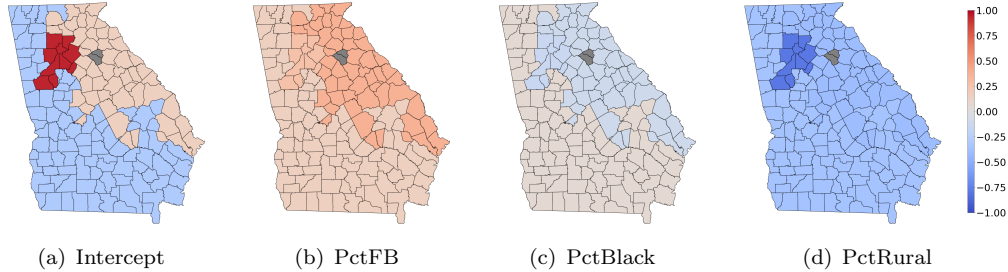


**Figure 9.** Estimated regression coefficients from the K-Models algorithm. The colors indicate the magnitude and direction of the effect (blue: negative; red: positive). Gray color is used to highlight a region with unreliable coefficient estimates.

OLS estimation, yet it does not suffice to produce reliable coefficient estimates. In the other three regions, an overall F-test of the regional regression model appears significant at 1% level. The effect of foreign born residents is positive, and slightly higher in the northern area. Rural residents has a negative effect across Georgia. The effect of African American is positive in the north, and negative in the south. Generally, these results are consistent with the results from GWR (Yu *et al.* 2020). Compared with GWR, our approach successfully detects the general pattern of coefficient variation, while capturing regional heterogeneity between three regions (along with one outlier region).

## 5. Discussion and conclusions

Regional modelling is a promising approach that accounts for both spatial heterogeneity and dependency, while finding an equilibrium between optimizing generality and accuracy of geographical models. We proposed a generalized regionalization framework, which extends the application of regionalization methods to various contexts including clustering, regression, and process modelling. This generalization work provides an approach to jointly delineate regions and make inference on processes underlying geographic phenomena beyond descriptive approaches that would focus on the form (Goodchild 2004, Fotheringham and Sachdeva 2022). Building on three existing regionalization algorithms, we extend their functionality to identify homogeneous regions given a dataset and a class of models. Instead of specifying a fixed region number  $K$ , we added a parameter  $\lambda$  to favor parsimonious models while providing some flexibility in the way model complexity is penalized. This approach also enables the use of spatial implicit regionalization algorithms. We demonstrate the effectiveness and usefulness of the proposed framework through spatial regression experiments on both simulated and real data.

Along with clustering and regression settings, our proposed framework is readily applicable to a wide range of geographic models. For example, the general gravity model (Getis 1991) is used to predict the spatial interaction flow between two places (Equation 17):

$$g_{k,l} = c \frac{p_k^a p_l^b}{d_{k,l}^\omega}, \quad (17)$$

where  $g_{k,l}$  is the estimated flow from place  $k$  to place  $l$ ;  $p_k, p_l$  are place sizes, represented

by population or GDP, for example;  $d_{k,l}$  is the distance between  $k$  and  $l$ ;  $a, b, c, \omega$  are model parameters. The gravity model can be calibrated for each spatial unit  $u_i$ , if a local interaction network  $G_i$  (a directed graph whose nodes are places in the unit, and the edge weight from node  $k$  to  $l$  is the observed interaction flow  $h_{k,l}$ ) is known. In this case, our framework can aggregate units with similar model parameters, and finally produce a regionalization scheme, with each region equipped with a set of parameters  $\theta = \{a, b, c, \omega\}$  (see Table 1). The gravity model can be calibrated with OLS after a logarithm transformation, or using an intelligent optimization method such as simulated annealing (Kirkpartick *et al.* 1983). Other complex models such as cellular automata or neural-network-based remote sensing image classifiers may be accommodated into our framework in a similar way. They may require specific fitting algorithms such as stochastic gradient descent for neural networks.

Spatial implicit methods for regionalization have been largely overlooked by the literature. Within a regression context, our results show that when the number of regions was not strictly restricted, the spatially implicit K-Models approach better reconstructed the regions both on simulated and real data. Inspired by a two-stage clustering approach, we suggested an automatic post-processing procedure to improve the K-Models algorithm in a regression application. This approach offers a wider range of improving moves during iteration, by relaxing the requirements on region connectivity. Afterwards, a post-processing procedure would merge redundant regions and ensure spatial contiguity in the final results. While our experiments illustrate the potential of our framework, future work would be required to carry out a comprehensive algorithm comparison. Furthermore, more work may be carried out to examine the performance of K-Models in attribute-based regionalization, regionalization for process modelling, and on data with different sizes and generating processes.

In many cases, calibration of regional models imposes a lower bound on the number of units in a region. In attribute-based regionalization, a region with only one or two units is not problematic. However, in the experiment on the Georgia dataset, at least four units are required to estimate regression coefficients and more units would be necessary to obtain more reliable estimates. More complex regression models, such as multi-layer perceptrons, would require a larger number of units to estimate the parameters. A possible remedy would be to consider small regions in the output as outliers. Yet within a multi-layer perceptron framework, this issue would need to be handled in the iteration process<sup>12</sup>. Instead of developing separate models for each regions, a global neural network with both shared and region-specific parameters (Xie *et al.* 2021) may be a promising way to integrate our framework with state-of-the-art GeoAI models, making the models aware of spatial heterogeneity by delineating corresponding regions.

We contributed to solve a puzzle of identifying regions whose models optimize both their ability to explain phenomena locally and globally. We argued that an optimal solution to delineate regions should consider both the parsimony and accuracy of models. Our work provided a perspective on the current discussion on replicability, or spatial generalization of geographical models. When we derive a model from data in one place, would it be applicable to other places? We suppose that an application scope should be determined for each model, out of which different models should be used. The result would be several regional models, which can be optimized in a top-down approach with the proposed framework. One major limitation of the proposed

---

<sup>12</sup>This is not problematic when each unit is associated with a dataset. In such cases, a model can be calibrated with data from a single unit (e.g. the gravity model introduced above).

framework is that the class of model cannot vary across regions. Future work may envisage allowing the use of different classes of models in different regions, which might find future applications.

### **Acknowledgements**

The acknowledgement is intentionally left blank for the peer-review process.

### **Data and codes availability statement**

The data and codes that support the findings of this study are available on a Github repository at <https://github.com/Nithouson/RegGeoModel>.

### **Disclosure statement**

The authors declare that they have no conflict of interest.

### **Funding**

This research was supported by grants from the National Natural Science Foundation of China (41830645, 41971331, 41771425), Smart Guangzhou Spatio-temporal Information Cloud Platform Construction (GZIT2016-A5-147), and the National Key Research and Development Program of China (2021YFC2701905).

### **Notes on contributors**

Hao Guo received his B.S. in Geographic Information Science and a dual B.S. in Mathematics from Peking University in 2020. He is currently a PhD student at Institute of Remote Sensing and Geographic Information System, Peking University. His research interests include spatial analysis, geo-spatial artificial intelligence, and spatial optimization.

Andre Python is ZJU100 Young Professor in Statistics at the Center for Data Science, Zhejiang University, P.R. China. He received his B.S. and M.S. from the University of Fribourg, Switzerland and his Ph.D from the University of St Andrews, United Kingdom. He develops and applies spatial models and interpretable machine learning algorithms to better understand the mechanisms behind the observed patterns of spatial phenomena.

Yu Liu is currently the Boya Professor of GIScience at the Institute of Remote Sensing and Geographic Information System, Peking University. He received his B.S., M.S., and Ph.D. degrees from Peking University in 1994, 1997, and 2003, respectively. His research interests mainly focus on humanities and social science based on big geo-data.

## References

- Anselin, L., 1988. *Spatial econometrics: methods and models*. Dordrecht: Kluwer Academic Publishers.
- Anselin, L., 2010. Thirty years of spatial econometrics. *Papers in Regional Science*, 89(1), 3–25.
- Assunção, R.M., et al., 2006. Efficient regionalization techniques for socio-economic geographical units using minimum spanning trees. *International Journal of Geographical Information Science*, 20(7), 797–811.
- Aydin, O., et al., 2021. A quantitative comparison of regionalization methods. *International Journal of Geographical Information Science*, 35(11), 2287–2315.
- Brunsdon, C., Fotheringham, A.S., and Charlton, M.E., 1996. Geographically weighted regression: a method for exploring spatial nonstationarity. *Geographical Analysis*, 28(4), 281–298.
- Clark, W.A.V., and Avery, K.L., 1976. The Effects of Data Aggregation in Statistical Analysis. *Geographical Analysis*, 8(4), 428–438.
- Duque, J.C., Ramos, R., and Suriñach, J., 2007. Supervised regionalization methods: A Survey. *International Regional Science Review*, 30(3), 195–220.
- Duque, J.C., Church, R.L., and Middleton, R.S., 2011. The p-Regions Problem. *Geographical Analysis*, 43(1), 104–126.
- Duque, J.C., Anselin, L., and Rey, S.J., 2012. The Max-p-Regions Problem. *Journal of Regional Science*, 52(3), 397–419.
- Feng, X., et al., 2021. pysal/spopt[software]. Available from: <https://github.com/pysal/spopt> [Accessed 29 October 2021]. doi: 10.5281/zenodo.4444156.
- Folch, D.C., and Spielman, S.E., 2014. Identifying regions based on flexible user-defined constraints. *International Journal of Geographical Information Science*, 28(1), 164–184.
- Fotheringham, A.S., 2020. Local modeling: one size does not fit all. *Journal of Spatial Information Science*, 21, 83–87.
- Fotheringham, A.S. and Brunsdon, C., 1999. Local Forms of Spatial Analysis. *Geographical Analysis*, 31(4), 340–358.
- Fotheringham, A.S. and Sachdeva, M., 2022. Modelling spatial processes in quantitative human geography. *Annals of GIS*, 28(1), 5–14.
- Fotheringham, A.S., and Wong, D.W.S., 1991. The modifiable areal unit problem in multivariate statistical analysis. *Environment and Planning A*, 23(7), 1025–1044.
- Fotheringham, A.S., Brunsdon, C., and Charlton, M., 2002. *Geographically weighted regression: the analysis of spatially varying relationships*. Hoboken: John Wiley & Sons.
- Fotheringham, A.S., Yang, W., and Kang, W., 2017. Multiscale Geographically Weighted Regression (MGWR). *Annals of the American Association of Geographers*, 107(6), 1247–1265.
- Gelman, A., and Hill, J., 2007. *Data Analysis Using Regression and Multilevel/Hierarchical Models*. Cambridge: Cambridge University Press.
- Getis, A., 1991. Spatial interaction and spatial autocorrelation: a cross-product approach. *Environment and Planning A*, 23, 1269–1277.
- Goodchild, M.F., 2004. GIScience, Geography, Form, and Process. *Annals of the Association of American Geographers*, 94(4), 709–714.
- Goodchild, M.F. and Li, W., 2021. Replication across space and time must be weak in the social and environmental sciences. *Proceedings of the National Academy of Sciences of the United States of America*, 118(35), e2015759118.
- Griffith, D.A., 2008. Spatial-Filtering-Based Contributions to a Critique of Geographically Weighted Regression (GWR). *Environment and Planning A*, 40(11), 2751–2769.
- Guo, D., 2008. Regionalization with dynamically constrained agglomerative clustering and partitioning (REDCAP). *International Journal of Geographical Information Science*, 22(7), 801–823.
- Harris, C.R., et al, 2020. Array programming with NumPy. *Nature* 585, 357–362.
- Karypis, G., Han, E.-H., and Kumar, V., 1999. Chameleon: Hierarchical Clustering Using Dynamic Modeling. *Computer*, 32(8), 68–75.
- Kirkpatrick, S., Gelatt, C., Vecchi, M., 1983. Optimization by Simulated Annealing. *Science*,



- 220, 671–680.
- Li, W., Church, R.L., and Goodchild, M.F., 2014. The p-Compact-regions Problem. *Geographical Analysis*, 46(3), 250–273.
- Liu, Y., et al, 2022. A note on GeoAI from the perspective of geographical laws. *Acta Geodaetica et Cartographica Sinica*, 51(6), 1062–1069.
- MacQueen, J., 1967. Some methods for classification and analysis of multivariate observations. *In: Proceedings of the Fifth Berkeley Symposium on Mathematical Statistics and Probability, Volume 1: Statistics*, Berkeley and Los Angeles: University of California Press, 281–296.
- Openshaw, S., 1977. A geographical solution to scale and aggregation problems in region-building, partitioning and spatial modelling. *Transactions of the Institute of British Geographers*, 2(4), 459–472.
- Openshaw, S., 1978. An empirical study of some zone design criteria. *Environment and Planning A*, 10(7), 781–794.
- Openshaw, S. and Rao, L., 1995. Algorithms for reengineering 1991 census geography. *Environment and Planning A*, 27(3), 425–446.
- Openshaw, S., and Wymer, C., 1995. Classifying and regionalizing census data. *In: S. Openshaw, ed. Census users' handbook*. Cambridge, UK: GeoInformation International, 239–270.
- Oshan, T. M., et al., 2019. MGWR: A python implementation of multiscale geographically weighted regression for investigating process spatial heterogeneity and scale. *ISPRS International Journal of Geo-Information*, 8, 269.
- Pedregosa, F., et al., 2011. Scikit-learn: Machine Learning in Python. *Journal of Machine Learning Research*, 12, 2825–2830.
- Rand, W.M., 1971. Objective Criteria for the Evaluation of Clustering Methods. *Journal of the American Statistical Association*, 66, 846–850.
- Rey, S.J., et al., 2021. The PySAL Ecosystem: Philosophy and Implementation. *Geographical Analysis*, in press, doi: 10.1111/gean.12276.
- Shaver, G.R., 2005. Spatial Heterogeneity: Past, Present, and Future. *In: Lovett, G.M., et al., ed. Ecosystem Function in Heterogeneous Landscapes*. New York, NY: Springer, 443–449.
- Sui, D., Kedron, P., 2021. Reproducibility and Replicability in the Context of the Contested Identities of Geography. *Annals of the American Association of Geographers*, 111(5), 1275–1283.
- Tobler, W.R., 1970. A Computer Movie Simulating Urban Growth in the Detroit Region. *Economic Geography*, 46(2), 234–240.
- Tong, D., Murray, A.T., 1970. Spatial optimization in geography. *Annals of the American Association of Geographers*, 102(6), 1290–1309.
- Vinh, N.X., Epps, J., Bailey, J., 2010. Information Theoretic Measures for Clusterings Comparison: Variants, Properties, Normalization and Correction for Chance. *Journal of Machine Learning Research*, 11, 2837–2854.
- Wang, J., Zhang, T., and Fu, B., 2016. A measure of spatial stratified heterogeneity. *Ecological Indicators*, 67, 250–256.
- Wei, R., Rey, S., and Knaap, E., 2021. Efficient regionalization for spatially explicit neighborhood delineation. *International Journal of Geographical Information Science*, 35(1), 135–151.
- Wei, R., Rey, S., and Grubestic, T.H., 2022. A Probabilistic Approach to Address Data Uncertainty in Regionalization. *Geographical Analysis*, 54, 405–426.
- Xie, Y., et al., 2021. Spatial-Net: A self-adaptive and model-agnostic deep learning framework for spatially heterogeneous datasets. *In: Proceedings of 29th International Conference on Advances in Geographic Information Systems (SIGSPATIAL'21)*, 2-5 November 2021 Beijing. New York: Association for Computing Machinery, 313–323.
- Xu, L., et al., 2011. Nonlinear effect of climate on plague during the third pandemic in China. *Proceedings of the National Academy of Sciences of the United States of America*, 108(25), 10214–10219.
- Yu, H., et al., 2020. Inference in Multiscale Geographically Weighted Regression. *Geographical Analysis*, 52(1), 87–106.

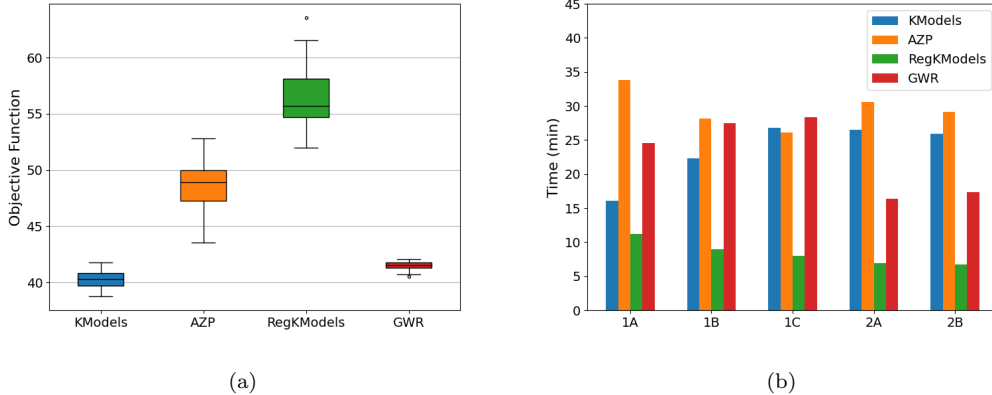


**Figure A1.** Results on algorithm stability and running time. (a) Boxplot showing the objective function values of solutions produced by four algorithms (K-Models (blue), AZP (orange), Regional-K-Models (green), and GWR (red)). Each algorithm is executed 50 times on a simulation from Dataset 2. (b) Average running time of each algorithm to carry out the simulated experiments. Three cases on Dataset 1 are labeled 1A (low noise,  $\sigma = 0.1$ ), 1B (medium noise,  $\sigma = 0.2$ ), and 1C (high noise,  $\sigma = 0.3$ ). Two cases on Dataset 2 is labeled 2A ( $\lambda = 5$ ) and 2B ( $\lambda = 3$ ). The times reported include multiple trials for different  $K$  values (2 to 20 for K-Models, AZP, and Regional-K-Models; 2 to 60 for GWR).

## Appendix A. Algorithm stability and running time

To examine the stability of the proposed zoning optimization algorithms, we take one simulation from Dataset 2, and repeat the regionalization process with each algorithm for 50 times. Figure A1a shows the distributions of objective function values. Even considering 50 repeats, no results from the spatially explicit methods, AZP and Regional-K-Models, are comparable with K-Models and GWR. Moreover, GWR and K-Models show less variability in repeating runs, indicating better stability compared to the spatially explicit methods. We infer that the merging process might have enhanced the algorithm stability. K-Models produces better solution than GWR in most cases but exhibits a slightly larger variability.

Figure A1b shows the running time of the four algorithms on simulated datasets. These algorithms took about ten minutes to half an hour to regionalize a  $25 \times 25$  grid. The time cost is considerably larger than attribute-based regionalization due to the larger time complexity associated with the model parameter estimation in a linear regression setting. Of the four algorithms, Regional-K-Models is the fastest and is considerably faster than AZP, as the latter considers a wider range of candidate moves. The time cost of K-Models is comparable with AZP and GWR.

## Appendix B. Discussion on the parameters $\lambda$ and $K$

In the proposed framework, the value of  $\lambda$  needs to be specified as input. This parameter is associated with the trade-off between the number of regions and the overall accuracy of the models. In practice, determining a suitable value of  $\lambda$  may be challenging. In some cases, we are only interested in a specific region scale (such as the region reconstruction experiment on Dataset 1 described in Section 4.1 and 4.2), and the optimal range of  $\lambda$  can be empirically identified with a relatively low number of trials. For users without any particular constraints on the region scale, we suggest

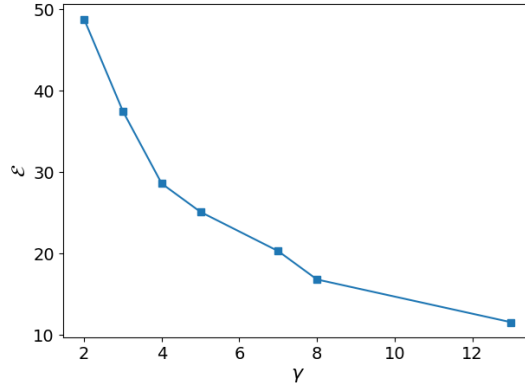
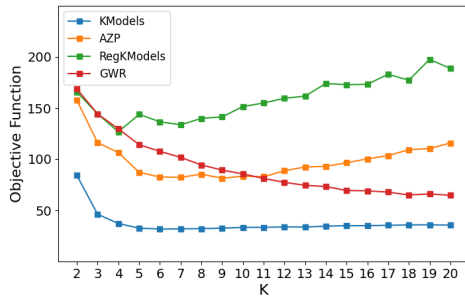


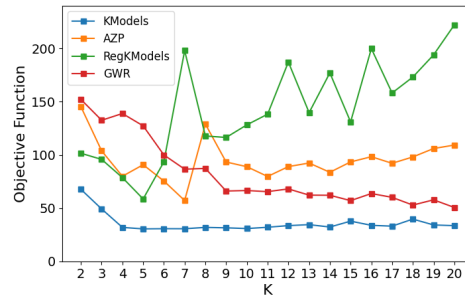
**Figure B1.** The estimated Pareto front for an experiment on a simulation from Dataset 2 using K-Models, with  $\lambda$  varying from 1 to 20. The markers stand for Pareto optimal solutions. The results reflect the trade-off between accuracy (minimizing the overall modelling error  $\mathcal{E}$ ) and generality (minimizing the number of regions  $\gamma$ ).

running the algorithms with different  $\lambda$  values, which will produce a range of possible results. Here the optimization problem can be viewed as multi-objective which jointly minimizes the modelling error  $\mathcal{E}$  and the number of regions  $\gamma$ . For each  $\gamma$ , we take the solution with the lowest modelling error  $\mathcal{E}$ . These solutions are called “Pareto optimal” (Tong and Murray 2012). The Pareto front is composed of all Pareto optimal solutions and reflects the trade-off between accuracy and generality. Figure B1 illustrates the estimated Pareto front from the K-Models algorithm, carried out on a simulation from Dataset 2, with  $\lambda = 1, 2, \dots, 20$ . As  $\lambda$  increases, the number of regions  $\gamma$  decreases from 13 to 2. All the Pareto solutions represent the heterogeneity of the spatial phenomenon at different region scales.

We investigate the effects of the input parameter  $K$  on Dataset 1 with a low noise (Figure B2). In this case, the true parameter distribution consists of five distinct regions. Although a series of  $K$  values could be tested, the choice of  $K$  is not that important in K-Models because of the merging procedure. Any choice of  $K$  from 5 to 20 produces satisfying result, as the algorithm merges the  $K$  initial regions into around 5 regions. The results for GWR show that the objective function decreases slowly with an increase in  $K$  on average. The best solution usually corresponds to a relatively large  $K$  value (between about 40 and 50). As for AZP and Regional-K-Models, the parameter  $K$  determines the number of produced regions. The best choice of  $K$  seems to be below 10 (4 for Regional-K-Models and 9 for AZP). As expected, the values of the objective function increases as  $K$  gets larger. Considering one run only, we note a relatively high variation in the objective function values associated with  $K$ , which seems to affect AZP and Regional-K-Models in particular (Figure B2b).



(a)



(b)

**Figure B2.** Effects of the parameter  $K$  on the objective function value for K-Models (blue), AZP (orange), Regional-K-Models (green), and GWR (red). (a) Mean objective function values at different  $K$  values from the experiment on 50 simulations in Dataset 1, with low noise ( $\sigma = 0.1$ ). (b) Objective function values for different  $K$  in one simulation in Dataset 1, with low noise.